Two-Phonon Production via Single-Phonon Scattering*

P. L. Leath and B. P. Watson
Department of Physics, Rutgers University, New Brunswick, New Jersey 08903
(Received 17 November 1970)

In recent numerical calculations of the one-phonon inelastic neutron scattering in Bravais quantum crystals, the existence of an extra unexplained peak in the scattering cross section has been reported. It is suggested here that this peak is due to two-phonon production via an intermediate virtual phonon. An analytic calculation in one dimension is done to derive a simple approximate dispersion rule $\omega_k^{(2)} \simeq 2\omega_{k/2}$ for these extra peaks. The possibility of the existence of two-phonon bound states or resonances is then considered and included analytically to show that the primary effect is to enhance the two-phonon production peak and shift its frequency.

I. INTRODUCTION

Recent, rather sophisticated, calculations of the one-phonon inelastic neutron scattering by very anharmonic crystals such as neon [1] and body-centered cubic helium [2] have demonstrated an unexplained additional peak (or neutron group) with a longitudinal polarization at frequencies above the usual phonon modes. This peak cannot represent an optical mode since these crystals are of the Bravais type. One purpose of this paper is to suggest that the additional peak can be produced by a resonance in the simple cubic-anharmonic bubble diagram [Fig. 1(a)] which corresponds, in a neutron-scattering experiment, to the process indicated by the diagram in Fig. 1(b) where a neutron (wavy line) scatters inelastically, producing a virtual phonon (solid line) that decays into two phonons via the cubic interaction. This simple diagram is common to the calculations of Goldman *et al.* [1] and Horner. [2] In the calculation by Goldman *et al.* [1] in neon, however, not only the simple bubble diagram but also the entire string of repeated bubbles [as shown in Fig. 1 (c)] were included; this class of diagrams is just that class which corresponds to the Born series for the mutual scattering of the two phonons via the quartic-anharmonic interaction, and which would show the existence of a bound state or resonance (if it exists) by a sharp peak. Similar phonon-phonon resonances (or roton-roton resonances) have recently been predicted and seen in liquid helium, [3] and in solids. [4] Thus, a second purpose of this work is to calculate this effect analytically and show that its dispersion throughout the Brillouin zone is not much different from that for the simple two-phonon production without the resonance, but that it can give an enhancement and shift in frequency of the simple two-phonon production peak.

We proceed in a manner somewhat unusual for quantum crystals, namely, by calculating the diagrams of interest by simple (non-self-consistent) perturbation theory. However, the purpose of this work is merely to direct the reader to the structure and physics lurking in the perturbation theory which, since the effects seem to persist in more sophisticated calculations, might be expected to be of some importance for real materials.

We calculate the diagrams shown in Fig. 1 analytically for a linear chain with nearest-neighbor forces. Our Hamiltonian is of the form

$$H=\sum_i \frac{p_i^2}{2M} + (2!)^{-1}\sum_{i,j}\Phi(i,j)u_i u_j + (3!)^{-1}\sum_{i,j,l}\Phi^{(3)}(i,j,l)u_i u_j u_l + (4!)^{-1}\sum_{i,j,l,m}\Phi^{(4)}(i,j,l,m)u_i u_j u_l u_m , \quad (1)$$

where p_i and u_i are the momentum and displacement of the ith atom, respectively, where M is the atomic mass, and where

$$\Phi(i,j)=\alpha_2[\delta_{i,j}-(\delta_{i+1,j}+\delta_{i,j+1})+\delta_{i+1,j+1}] , \quad (2a)$$

$$\Phi^{(3)}(i,j,l)=\alpha_3[\delta_{i,j,l}-(\delta_{i+1,j,l}+\delta_{i,j+1,l}+\delta_{i,j,l+1}) + (\delta_{i+1,j+1,l}+\delta_{i+1,j,l+1}+\delta_{i,j+1,l+1})-\delta_{i+1,j+1,l+1}] , \quad (2b)$$

and

$$\Phi^{(4)}(i,j,l,m)=\alpha_4[\delta_{i,j,l,m} - (\delta_{i+1,j,l,m}+\cdots)+(\delta_{i+1,j+1,l,m}+\cdots) - (\delta_{i+1,j+1,l+1,m}+\cdots)+\delta_{i+1,j+1,l+1,m+1}] \quad (2c)$$

are the harmonic, cubic-anharmonic, and quartic-anharmonic force constants, respectively, where $\delta_{i,j,l,\ldots}$ is the quasi-Kronecker-delta which is 1 whenever $i=j=l=\circ\ldots$, and zero otherwise. The Fourier components of these force constants are

$$\Phi(k)=4\alpha_2\sin^2\tfrac{1}{2}ka=M\omega_m^2\sin^2\tfrac{1}{2}ka=M\omega_k^2 , \quad (3a)$$

and, generally,

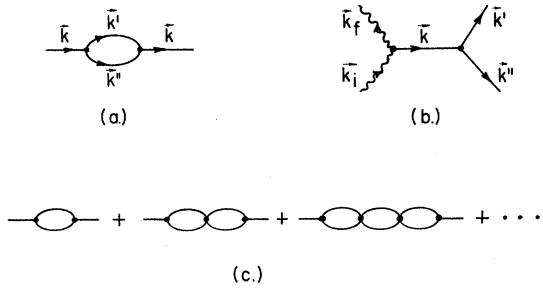

FIG. 1. Simple cubic-anharmonic bubble diagram (a) corresponding to the physical process (b) where a neutron (wavy line) scatters inelastically, producing a virtual phonon (solid line) that decays into two phonons by the cubic-anharmonic interaction. The repeated scattering of two phonons by the quartic-anharmonic interaction (c) which can lead to two-phonon bound states.

$$\Phi^{(n)}(k_1, k_2, \ldots, k_n) = (2i)^n \alpha_n \sin\tfrac{1}{2}k_1 a \sin\tfrac{1}{2}k_2 a \times \cdots \sin\tfrac{1}{2}k_n a\, e^{i(k_1+k_2+\cdots+k_n)a/2}\Delta(k_1+k_2+\cdots+k_n), \tag{3b}$$

where $\Delta = 1$ whenever $k_1+k_2+\cdots+k_n = K$, a reciprocal-lattice vector, and where the exponential factor is thus always $+1(-1)$ for even- (odd-) order umklapp processes (this factor always appears squared and thus never matters in the processes considered here).

We calculate the one-phonon retarded Green's function[5] defined in configuration space by

$$G(n, m, t-t') = \frac{1}{i\hbar}\langle[u(n, t), u(m, t')]\rangle_T \theta(t-t') = \langle\langle u(n, t); u(m, t')\rangle\rangle , \tag{4}$$

where $\langle[\ldots,\ldots]\rangle_T$ is the thermal average of the commutator. It is $\mathrm{Im}[G(k, \omega)]$ which gives the one-phonon inelastic neutron scattering directly. The harmonic value $g(k, \omega)$ of the Fourier components of Eq. (4) are given by

$$g(k, \omega) = M^{-1}(\omega^2 - \omega_k^2)^{-1} . \tag{5}$$

In each case below, we calculate the phonon self-energy defined by the equation

$$G(k, \omega) = \frac{g(k, \omega)}{1 - g(k, \omega)\Sigma(k, \omega)} = \frac{1}{M[\omega^2 - \omega_k^2 - M^{-1}\Sigma(k, \omega)]} . \tag{6}$$

II. SIMPLE TWO-PHONON PRODUCTION

The lowest-order anharmonic term in $\Sigma(k, \omega)$ which has an interesting frequency dependence is that corresponding to the simple bubble diagram in Fig. 1(a), which is shown in Appendix A to be of the matrix form

$$\Sigma(\omega) = \tfrac{1}{4}\underline{\Phi}^{(3)} : \underline{g}^{(2)}(\omega) : \underline{\Phi}^{(3)} , \tag{7}$$

where $\underline{g}^{(2)}$ is the harmonic value of the two-phonon Green's function

$$G^{(2)}(n, n'; m, m', t) = \frac{1}{i\hbar}\langle[u(n, t)u(n't), u(m, 0)u(m', 0)]\rangle_T \theta(t) , \tag{8}$$

which decouples exactly in the harmonic approximation into

$$g^{(2)}(n, n'; m, m', t) = f(n, m', t)g(n', m, t) + f(n, m, t)g(n', m', t) + g(n, m', t)f(m, n', -t) + g(n, m, t)f(m', n', -t) , \tag{9}$$

where $f(n, m, t) = \langle u(n, t)u(m, 0)\rangle_T$ is the one-phonon correlation function. Thus, the Fourier components of Eq. (9) are given by the convolution

$$g^{(2)}(k, k', k_1, k_2, \omega) = [\Delta(k, k_1)\Delta(k', k_2) + \Delta(k, k_2)\Delta(k', k_1)] \times \int_{-\infty}^{\infty} [f(k, z)g(k', \omega - z) + g(k, \omega - z)f(k', -z)]\, dz . \tag{10}$$

This convolution integral is trivial since $f(k, z)$ has the δ-function behavior[5]

$$f(k, z) = \frac{-[n(z)+1]\hbar}{\pi}\mathrm{Im}[g(k, z)] = \frac{[n(z)+1]\hbar}{2Mz}[\delta(z-\omega_k) + \delta(z+\omega_k)] , \tag{11}$$

where $n(z) = (e^{\hbar z/kT} - 1)^{-1}$, the Planck distribution function, and we have used Eq. (5). When we put this result into Eq. (7) in the k representation

$$\Sigma(k, \omega) = -\frac{1}{4N} \times \sum_{k', k''} |\Phi^{(3)}(k, k', k'')|^2 g^{(2)}(k', k'', \omega) , \tag{12}$$

we find

$$\Sigma(k, \omega) = -\frac{1}{4N}\sum_{k', k''} |\Phi^{(3)}(k, k', k'')|^2 \frac{\hbar}{2M^2\omega_{k'}\omega_{k''}} \times \left(\frac{(n_{k'}+n_{k''}+1)}{\omega+\omega_{k'}+\omega_{k''}} - \frac{(n_{k'}+n_{k''}+1)}{\omega-\omega_{k'}-\omega_{k''}} + \frac{(n_{k''}-n_{k'})}{\omega+\omega_{k'}-\omega_{k''}} + \frac{(n_{k'}-n_{k''})}{\omega+\omega_{k''}-\omega_{k'}}\right) . \tag{13}$$

This result is also easily obtained directly from the diagram rules.[6]

We then evaluate $\Sigma(k, w)$ by putting Eq. (3) into (13), but first we make two changes. We set $T=0$, which has the effect of setting $n_{k'}=n_{k''}=0$, thereby removing the phonon bath and the last two terms in (13) which correspond to the emission and absorption of one phonon. The essential two-phonon production remains. Also we let the number of atoms $N\to\infty$ and replace $N^{-1}\sum_k(\ldots)$ by the integral

$$(a/2\pi)\int_{-\pi/a}^{\pi/a} dk(\ldots)\ .$$

Thus we obtain

$$\Sigma(k,\ \Omega)=-\frac{4\hbar\alpha_3^2\sin^2(\frac{1}{2}ka)a}{\pi M^2\omega_m^3}\int_{-\pi/a}^{\pi/a} dk'\,|\sin\tfrac{1}{2}k'a|\,|\sin\tfrac{1}{2}(k-k')a| \times\left(\frac{1}{\Omega+|\sin\frac{1}{2}(k-k')a|+|\sin\frac{1}{2}k'a|}+\frac{1}{|\sin\frac{1}{2}(k-k')a|+|\sin\frac{1}{2}k'a|-\Omega}\right), \quad (14)$$

where $\Omega=\omega/\omega_m$ and the absolute values are necessary because ω_k is always positive.[7] We eliminate the need for the absolute value on $\sin\frac{1}{2}k'a$ very simply by shifting the range of integration from $(-\pi/a,\ \pi/a)$ to $(0,\ 2\pi/a)$, which is allowed since the integrand of (14) is periodic in $2\pi/a$. The remaining absolute value on $\sin\frac{1}{2}(k-k')a$ is then removed simply by breaking the remaining integral into two parts

$$\int_0^k dk'(\ldots)+\int_k^{2\pi/a} dk'(\ldots)\ .$$

With a little manipulation, $\Sigma(k,\ \omega)$ is thus put in the form

$$\Sigma(k,\ \Omega)=\frac{-4\hbar\alpha_3^2\sin^2(\frac{1}{2}ka)a}{\pi M^2\omega_m^3} \times\left[I(k,\ \Omega)+I(k,\ -\Omega)+I\left(k-\frac{2\pi}{a},\ -\Omega\right)+I\left(k-\frac{2\pi}{a},\ \Omega\right)\right], \quad (15)$$

where

$$I(k,\ \Omega)=\int_0^k \frac{dk'\sin(\frac{1}{2}k'a)\sin\frac{1}{2}(k-k')a}{\Omega+\sin(\frac{1}{2}k'a)+\sin\frac{1}{2}(k-k')a}\ . \quad (16)$$

This integral, actually $[I(k,\ \Omega)+I(k,\ -\Omega)]$, is evaluated in a straightforward manner in Appendix B, with the result

$$\Sigma(k,\ \Omega)=-M\omega_m^2\gamma\sin^2(\tfrac{1}{2}ka)F(k,\ \Omega)\ , \quad (17)$$

where

$$F(k,\ \Omega)=2+\tfrac{1}{2}(\Omega^2-\sin^2\tfrac{1}{2}ka)[A(\cos\tfrac{1}{2}ka,\ \Omega^2)+A(-\cos\tfrac{1}{2}ka,\ \Omega^2)] \quad (18b)$$

and

$$A(\cos\tfrac{1}{2}ka,\Omega^2)=\begin{cases} B^{-1/2}C^{-1}[\ln|(C+B^{1/2})/(C-B^{1/2})|-\pi i\theta(\omega^2-\omega_k^2)] & \text{for } B>0 \\ -2(-B)^{-1/2}C^{-1}\tan^{-1}C(-B)^{-1/2} & \text{for } B<0\ , \end{cases} \quad (18b)$$

with $C=1-\cos\frac{1}{2}ka$, $B=2C-\Omega^2$, and $\gamma=16\hbar\alpha_3^2/(M^3\omega_m^5\pi)$, a dimensionless parameter.

The real (solid line) and imaginary (dashed line) parts of $(M\omega_m^2)^{-1}\Sigma(k,\ \omega)$ in Eq. (17) are plotted in Figs. 2(a) and 2(c) for $\gamma=0.3$ (a value corresponding, in order of magnitude, to the anharmonicity of neon[8]) vs $\Omega=\omega/\omega_m$ for $k=0.6\,\pi/a$ and $0.9\,\pi/a$.

The imaginary part of $\Sigma(k,\ \omega)$ is nonzero only along the two branch cuts of the weighted two-phonon Green's function $F(k,\ \Omega)$ (or the joint density of states), which from Eq. (13) is in the region where $\omega=\omega_{k'}+\omega_{k-k'}$ can be satisfied. In Fig. 3 we sketch $\omega_{k'}+\omega_{k-k'}$ vs k' for a given value of k. From this sketch it is clear that the two-phonon density of states extends throughout two overlapping branch cuts in the frequency intervals $(\omega_k,\ 2\omega_{k/2})$ and $(\omega_k,\ 2\omega_{(k-K)/2})$, where $K=2\pi/a$ is a reciprocal-lattice vector. The lower branch points are such that $\mathrm{Im}[\Sigma(k,\ \omega)]$ is zero for $\omega<\omega_k$ (and thus does not give a lifetime to the ordinary phonon peak); this result is because a finite energy is required to create two phonons (Maris has previously pointed out this fact[9]) and will disappear for $T>0$, where the last two terms in Eq. (13) contribute. At the two upper branch points (at $2\omega_{k/2}$ and $2\omega_{(k-K)/2}$), the dispersion curve in Fig. 3 is flat so that there is a critical point in the joint density of states and $-\mathrm{Im}[\Sigma(k,\ \omega)]$ diverges at these points. This feature is evident in the result (18) which diverges at $B=0$, where

$$\omega=\omega_k^{(2)}=\sqrt{2}\,\omega_m[1\pm\cos\tfrac{1}{2}ka]^{1/2}$$

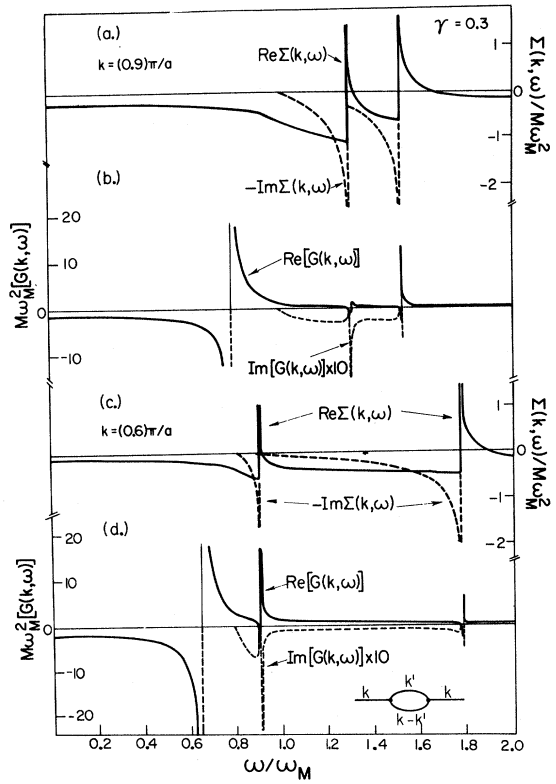

FIG. 2. Real (solid line) and imaginary (dashed line) parts of $\Sigma(k, \omega)$ and $G(k, \omega)$ vs ω for two values of k, as given by Eq. (6) and (17). The diagram in the lower right-hand corner represents the process considered here.

$$= 2\omega_m \left| \sin\tfrac{1}{4}(k - 2n\pi/a)a \right| = 2\omega_{(k-2n\pi/a)/2} \,. \quad (19)$$

A similar effect will occur in three-dimensional systems at critical points of the saddle-point type, although the joint density of states will remain finite.

In the linear chain, the real part of $\Sigma(k, \omega)$ in (17) also diverges but on the high-frequency side of the critical points at $\omega_k^{(2)}$. This produces two resonances in $G(k, \omega)$, in Eq. (6), as plotted in Figs. 2(b) and 2(d), at frequencies just beyond $\omega_k^{(2)}$, where the resonance condition

$$M\omega^2 = M\omega_k^2 - \mathrm{Re}[\Sigma(k, \omega)] = 0 \quad (20)$$

is satisfied. This condition, although always satisfied at some frequency in the linear chain, cannot always be satisfied in three-dimensional systems because $\mathrm{Re}[\Sigma(\vec{k}, \omega)]$ does not become infinite and thus (depending upon the coupling constant α_3^2) might not become as large as $M(\omega^2 - \omega_{\vec{k}}^2)$. Two possible cases are sketched in Fig. 4 at frequencies just above the critical-point peaks in the two-phonon density of states where the real part of $\Sigma(\vec{k})$ has a peak. In the case of small α_3^2, or small anharmonicity, the real part of $\Sigma(\vec{k}, \omega)$ (dashed line) never crosses $M(\omega^2 - \omega_{\vec{k}}^2)$ (solid line), so that Eq. (20) is never satisfied and no resonance appears. However, for large α_3^2, the peak in the real part of $\Sigma(\vec{k}, \omega)$ (dotted line) crosses $M(\omega^2 - \omega_{\vec{k}}^2)$ and a resonance develops. Actually, in this latter case $\mathrm{Re}[\Sigma(\vec{k}, \omega)]$ crosses $M(\omega^2 - \omega_{\vec{k}}^2)$ twice; the lower crossing is an antiresonance since $\mathrm{Im}[\Sigma(\vec{k}, \omega)]$ is so large here, but the higher crossing is a true resonance and can be very sharp.

There is some interference between the two peaks which is striking because the imaginary part of $\Sigma(k, \omega)$ is only large on the low-frequency side of $\omega_k^{(2)}$. For the lowest two-phonon peak, there is a finite lifetime coming from the tail of $\mathrm{Im}[\Sigma(k, \omega)]$ from the upper critical point, whereas (in this calculation) the upper two-phonon peak has an infinite lifetime (which will undoubtedly be modified by higher-order terms). This asymmetry causes a growing of the lower-frequency peak relative to the upper one as k tends to zero and the two poles separate. It should also be noted that $\Sigma(k, \omega)$ in Eq. (15) reduces as k tends away from the Brillouin zone toward zero (since it is proportional to $\sin^2\frac{1}{2}ka$ coming from the virtual phonon which is the weak link in this process) and both resonances disappear. In three dimensions the resonance might only exist near the Brillouin-zone edge.

Perhaps the most important feature of the calculation is the dispersion curve of the poles in $G(k, \omega)$ which are shown by the solid curves in Fig. 5. The dashed curve is the harmonic frequency $\omega_M \sin\frac{1}{2}ka$, the lowest solid curve is the shifted single-phonon pole, and the upper two branches represent the two-phonon production resonances near $\omega_k^{(2)} = 2\omega_{k/2}$ and $2\omega_{(k-2\pi/a)/2}$. The uppermost curve at $2\omega_{(k-2\pi/a)/2}$ can be thought of as an umklapp branch where two phonons of $k > \pi/2a$ are created and travel in a direction opposite to that of the virtual phonon. The

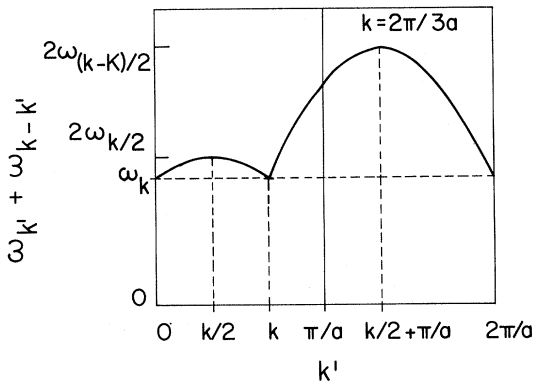

FIG. 3. Two-phonon dispersion curve $\omega_{k'} + \omega_{k-k'} = \sin(\frac{1}{2}k'a) + \sin((\frac{1}{2}k - k')a)$ plotted vs k' for a typical value of k. The critical points in the two-phonon density of states correspond to the places of zero slope.

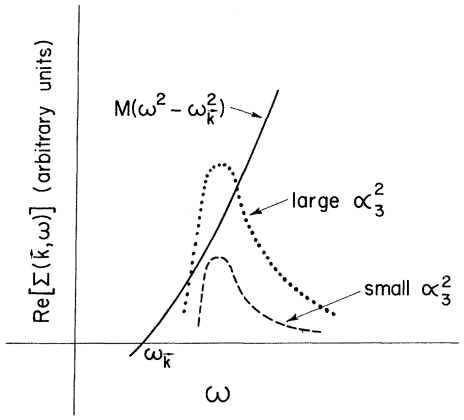

FIG. 4. Sketch of $\mathrm{Re}[\Sigma(k,\omega)]$ vs ω, as it might be expected to appear in three-dimensional systems for small (dashed line) and large (dotted line) values of α_3^2, and $M(\omega^2-\omega_k^2)$ (solid line) vs ω. The crossing of the curves corresponds to solutions of Eq. (20). A similar situation results for solutions of $1-\eta F(k,\Omega)=0$ which is a phonon-phonon resonance as is discussed below Eq. (25).

two branches are degenerate at the Brillouin-zone boundary, a degeneracy probably broken by higher-order interactions. For $k\to 0$ the umklapp branch goes to $2\omega_m$, whereas the normal two-phonon branch goes to $2\omega_{k/2}=2(\frac{1}{2}ck)=ck$, the single harmonic-phonon branch as the dispersion disappears. Actually, in a self-consistent calculation, the normal two-phonon branch will become tangent to the true one-phonon curve as $k\to 0$.

In three-dimensional systems, such resonances will appear if $\mathrm{Re}[\Sigma(\vec{k},\omega)]$ becomes as large as $M\omega^2-M\omega_{\vec{k}}^2$ near the critical points of the two-phonon density of states. It might be the case that there are resonances only in certain symmetry directions where $\mathrm{Re}[\Sigma(\vec{k},\omega)]$ is larger due to more $\vec{k}$ space within the Brillouin zone about that direction (for example, for k near zone faces rather than near zone corners). Also, the simple dispersion rule $\omega_{\vec{k}}^{(2)}\simeq 2\omega_{(\vec{k}-\vec{K})/2}$ might not be expected to hold along certain symmetry directions due to the phonon frequencies off the symmetry direction.

It seems clear that the above explanation is likely to be the cause of the extra peaks observed by Horner[2] in solid bcc helium, since, except for self-consistent renormalizations, Horner has calculated just the simple cubic-anharmonic bubble diagram of Fig. 1(a). In Fig. 6, we show the dispersion curves of helium for longitudinal phonons along the [100] and [110] direction as calculated by Horner. Superimposed (dashed line) are the values of $2\omega_{\vec{k}/2}$ and $2\omega_{(\vec{k}-\vec{K})/2}$, where his values of $\omega_{\vec{k}}$ have been used. The agreement with his extra peak is remarkable considering the formula can only be qualitative for three-dimensional systems. Horner does not report the extra umklapp peak, presumably either because he did not study this frequency range or because this peak disappears rapidly as $\vec{k}$ tends to zero. Also, there seems to be no fundamental reason why such peaks might not also occur for transverse branches.

For neon, Goldman *et al.*[1] also report an additional peak at the Brillouin-zone edge. They have also included, however, the quartic phonon-phonon interaction bubbles in Fig. 1(c), so we thought, perhaps, their peak could be explained via a phonon-phonon resonance or bound state. The position of their extra peak is somewhat below the simple dispersion law $\omega_{\vec{k}}^{(2)}=2\omega_{\vec{k}/2}$ even though, perhaps, it is not inconsistent with the simple explanation above (it being a three-dimensional system). Therefore, in Sec. III we calculate analytically, for our model, the effect of a phonon-phonon bound state on the two-phonon production peak. Inelastic-neutron-scattering experiments are presently in progress to look for these extra peaks in neon.[10]

It should be noted at this point that Cowley has previously suggested that structure in the real and imaginary parts of $\Sigma(\vec{k},\omega)$ due to the two-phonon Green's function could give rise to structure in the neutron-scattering cross section.[11] This is actually what is being suggested here in a somewhat more dramatic fashion.

The new suggestion here is that two acoustic phonons can be produced via an intermediate virtual acoustic phonon. This particular process is absent at $k=0$ due to the virtual acoustic phonon and hence is not observable by optical experiments. Nevertheless, closely related processes have been ob-

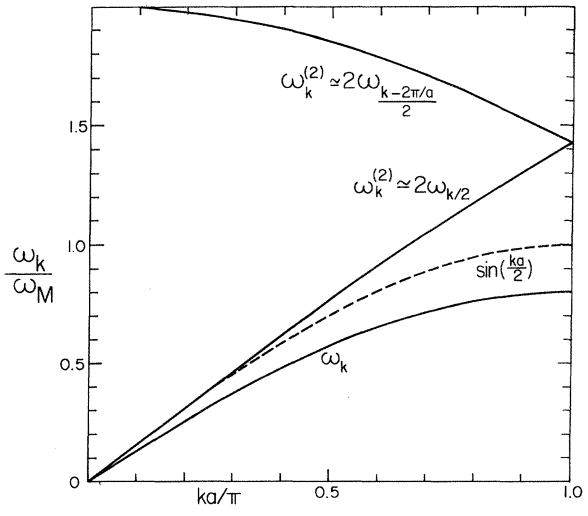

FIG. 5. Dispersion curves (solid line) of the poles in $G(k,\omega)$ vs k for the simple two-phonon production (the lowest curve is the frequency-shifted single-phonon curve) and the harmonic pole (dashed line).

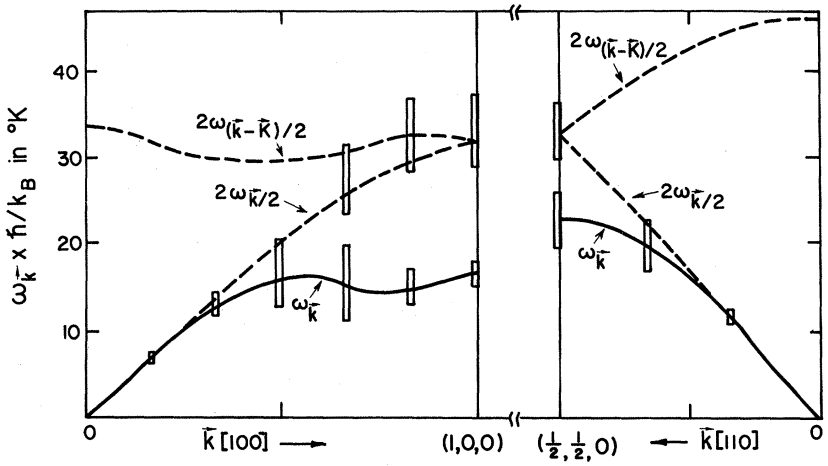

FIG. 6. Phonon dispersion curves (solid lines) of bcc helium as calculated by Horner in Ref. 2, including his additional peak (the vertical bars give its width), and superimposed, the naive $\omega_{\vec{k}}^{(2)} = 2\omega_{(\vec{k}-\vec{K})/2}$ formula for the two-phonon peaks.

served in polyatomic crystals involving an optic virtual phonon in quartz[12] and involving librons in solid hydrogen.[13] Furthermore, the resonances calculated here are produced by structure in the two-phonon density of states and hence essentially coincide with direct two-phonon production processes such as in second-order optical experiments[14] and in two-phonon inelastic neutron scattering. A related process whereby two phonons are produced directly which subsequently merge into a single phonon has been considered by Ambegaokar *et al.*[15] and will also coincide with the above processes experimentally. These authors estimated the size of their terms and decided that they were small enough not to be resolvable by inelastic neutron scattering for lead,[15] which must also be true for the process calculated here. Perhaps, however, more anharmonic materials such as helium and neon will exhibit these peaks, as seems possible since they were easily resolvable in the calculations of Refs. 1 and 2.

Finally, it should be noted that, although we have restricted our discussion so far to two-phonon production, the qualitative effect of n-phonon production is easily discovered. In n-phonon production, the resonance, if it exists, is produced by structure in the n-phonon Green's function. The peaks, or critical points, in the n-phonon Green's function are easily analyzed for our linear chain model. They occur at extrema in the dispersion curve of

$$\omega_{k_1} + \omega_{k_2} + \cdots + \omega_{k_{n-1}} + \omega_{k-(k_1+k_2+\cdots+k_{n-1})}, \tag{21}$$

the quantity which appears in the denominator of the n-phonon Green's function, plotted versus k_1, $k_2, \ldots, k_{n-1}$. Writing $\omega_k = \omega_m \sin\frac{1}{2}ka$ and setting all the partial derivatives of (21), with respect to k_1, $k_2, \ldots, k_{n-1}$, equal to zero gives immediately that the critical points of $g^n(\omega)$ occur at

$$\omega_k^{(n)} = n\omega_{(k-K)/n}, \tag{22}$$

where K is any reciprocal-lattice vector. The lowest branch of n production occurs at a frequency $\omega_k^{(n)} = n\omega_{k/n}$ which lies (for all n) between the one-phonon dispersion curve and the straight-line tangent at $k=0$ with the velocity of sound. Thus, in this lowest branch at $n\omega_{k/n}$, the multiphonon production (for all n) get crowded into a relatively small region. Nevertheless, these higher-order terms probably are small.

III. TWO-PHONON PRODUCTION WITH PHONON-PHONON RESONANCE

It has been predicted and reported that phonon-phonon (or roton-roton) bound states or resonances exist in liquid helium[3] and in anharmonic solids.[4] Recently, Ruvalds has suggested they also might exist in solid helium.[16] Therefore, it is instructive to calculate analytically the effect of a possible phonon-phonon resonance on the two-phonon production peak. This effect requires summing the class of diagrams shown in Fig. 1(c) where the two phonons repeatedly interact via the quartic interaction. This class of diagrams has also been summed by Goldman *et al.*[1] in their neon calculation. This calculation proceeds in the same manner as that of Sec. II by letting $T=0$ (so that the calculation can be done analytically) and neglecting those processes which are not of direct interest here.

The self-energy Σ_R including those diagrams of Fig. 1(c) can be derived by using an equation-of-motion technique (including quartic terms) similar to that described in Appendix A for the two-phonon Green's function in Eq. (A5) that appears in the self-energy. Neglecting all terms except those that give repeated bubbles, one finds, in matrix notation,

$$\Sigma_R(\omega) = \tfrac{1}{4}\underline{\Phi}^{(3)} : \underline{g}^{(2)}(\omega) : \underline{\Phi}^{(3)}$$

$$+ \tfrac{1}{4}(1/3!)\underline{\Phi}^{3} : \underline{g}^{(2)} : \underline{\Phi}^{(4)} : \underline{g}^{(2)} : \underline{\Phi}^{(3)} + \tfrac{1}{4}(1/3!)^2 \underline{\Phi}^{(3)} : \underline{g}^{(2)} : \underline{\Phi}^{(4)} : \underline{g}^{(2)} : \underline{\Phi}^{(4)} : \underline{g}^{(2)} : \underline{\Phi}^{(3)} + \cdots , \quad (23)$$

where the colon indicates a double contraction on the indices. In k representation the matrix elements of (23) are (except for umklapp scattering for the moment)

$$\Sigma_R(k,\omega) = -\frac{1}{4N}\sum_{k_1} \Phi^{(3)}_{k,k_1} g^{(2)}_{k_1}\left[\Phi^{(3)}_{k,k_1} + \frac{1}{6N}\sum_{k_2} \Phi^{(4)}_{k_1,k_2} g^{(2)}_{k_2} \times \left(\Phi^{(3)}_{k,k_2} + \frac{1}{6N}\sum_{k_3} \Phi^{(4)}_{k_2,k_3} g^{(2)}_{k_3} \Phi^{(3)}_{k,k_3} + \cdots\right)\right], \quad (24)$$

where $g^{(2)}_{k_1}$, $\Phi^{(3)}_{k,k_1}$, and $\Phi^{(4)}_{k_1,k_2}$ are short notations for $g^{(2)}_{(k_1,k-k_1,\omega)}$, $\Phi^{(3)}_{(-k,k_1,k-k_1)}$, and $\Phi^{(4)}_{(-k_1,k_1-k,k_2,k-k_2)}$, respectively. This series is geometric and simple to sum for our linear chain model since both $\Phi^{(3)}$ and $\Phi^{(4)}$ are separable in Eq. (3b), after the δ function is satisfied. Thus we find immediately (as $N \to \infty$) that Eq. (24) becomes simply Eq. (17) with a denominator, or

$$\Sigma_R(k,\Omega) = \frac{-M\omega_m^2 \gamma \sin^2(\frac{1}{2}ka)\, F(k,\Omega)}{1-\eta F(k,\Omega)}, \quad (25)$$

where

$$\eta = 16\hbar\alpha_4/(6\pi M^2\omega_m^3),$$

and where $F(k,\Omega)$ is defined in Eq. (18), which is the weighted two-phonon Green's function that we have evaluated above and which gave us the structure before.

Thus, we plot $\Sigma_R(k,\omega)$ in Fig. 7 for $\eta = +0.5$, a value (a few times larger than the value for neon[8]) which was chosen to clearly illustrate the effect of the phonon-phonon bound state. The value of η must be positive (corresponding to repulsive forces) to produce a phonon-phonon bound state, since the phonon-dispersion curve has a negative curvature corresponding to a negative effective mass. Figure 7 contains a repetition of the calculations shown in Fig. 2 for the simple two-phonon production, but including the denominator $[1-\eta F(k,\Omega)]$ in $\Sigma(k,\Omega)$ as in Eq. (25).

Perhaps the most striking feature is that the phonon-phonon bound state shifts the two-phonon pole in $G(k,\omega)$ only very slightly (to order α_4) from its frequency in the simple two-phonon production. This result is because the two-phonon bound state (and hence the pole) occurs very near the same peak in the two-phonon Green's function $F(k,\Omega)$ that produced the previous structure. A situation similar to that in Fig. 4 again results in three-dimensional systems where the phonon-phonon resonance occurs where $F(k,\Omega)$ (like the dashed line in Fig. 4) crosses the horizontal line of value one. Therefore, we do not plot the new dispersion curve for the two-phonon poles in $G(k,\Omega)$ because they are shifted very little (the order of 1%) and stay near $2\omega_{(k-K)/2}$ in our linear chain. The small shift caused by this resonance is in such a direction as to shift the lower two-phonon peak to lower frequencies and the upper peak to higher frequencies. It should be noted, on the other hand (as is evident by comparing Figs. 2 and 7), that the single-phonon frequency is shifted upward significantly (about 10%) by the phonon-phonon resonance.

The phonon-phonon resonance always occurs at some frequency in the linear chain model, because $1-\eta F(k,\Omega) = 0$ can always be satisfied.

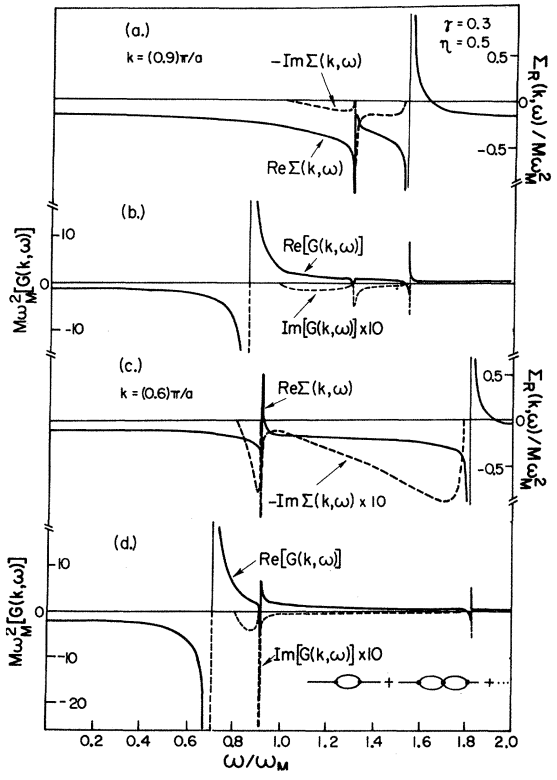

FIG. 7. Real (solid line) and imaginary (dashed line) parts of $\Sigma(k,\omega)$ and $G(k,\omega)$ vs ω, for two values of k, as given by Eqs. (6) and (25). The diagram in the lower right-hand corner represents the process considered here.

This is because the two-phonon Green's function becomes infinite at its critical points. In three-dimensional systems this behavior will not always be the case and a critical value of α_4 will be necessary to produce the bound state. From the numerical calculations of Goldman, Horton, and Klein, it seems there is no phonon-phonon resonance in neon, although the simple two-phonon production resonance does appear clearly.[8] It is possible, however, that phonon-phonon resonances do exist in solid helium. The effect of the phonon-phonon resonance on the two-phonon production peak is primarily to enhance it (or, perhaps, to make it appear, if α_3 is small and α_4 is large enough to produce the resonance). It usually seems that the cubic (α_3^2) and quartic (α_4) anharmonicity are about the same order of magnitude and the two effects discussed here appear nearly simultaneously.

It would seem nearly impossible by one-phonon inelastic neutron scattering to conclude that the phonon-phonon resonance or bound state exists, even if these extra peaks are seen.

However, direct two-phonon production can be greatly enhanced by the phonon-phonon resonance. Second-order optical experiments such as those of Ref. 4 clearly seem to be the best tool for this measurement since they also have the resolution to measure the shift (of order α_4) in the two-phonon production or the phonon-phonon binding energy.

Finally, it should be noted that an η of the wrong sign will attenuate or destroy the two-phonon production peak in contrast to the enhancement described above.

Note added in proof. R. A. Reese, S. K. Sinha, T. O. Brun, and C. R. Tilford (unpublished) have recently studied the inelastic neutron scattering by hcp helium and report considerable structure in the neutron groups at high frequencies which seems likely to be due to two—or higher—phonon production that might be explainable by structure in the two-phonon Green's function as discussed here.

ACKNOWLEDGMENTS

We gratefully acknowledge many stimulating and important discussions of this problem with our colleagues at Rutgers. In particular, we are indebted to Professor G. K. Horton for bringing the problem of the additional peak to our attention. We should also like to thank Professor J. A. Krumhansl and Professor J. Ruvalds for useful comments on a preliminary version of the manuscript.

APPENDIX A

In this appendix we derive the self-energy $\Sigma(k,\omega)$ corresponding to the simple bubble diagram of Fig. 1(a) by an equation-of-motion technique. We first differentiate Eq. (4) with respect to t to obtain

$$\frac{\partial G(n,m,t-t')}{\partial t} = \frac{1}{M}\langle\langle p(n,t);u(m,t')\rangle\rangle$$

$$= \frac{1}{i\hbar M}\langle[p(n,t),u(m,t')]\rangle_T\,\theta(t-t'), \quad \text{(A1)}$$

where we have used the equation of motion

$$\frac{\partial u(n)}{\partial t} = (i\hbar)^{-1}[u(n),H] = \frac{p(n)}{M},$$

which follows from the Hamiltonian (1). Then differentiating again,

$$\frac{\partial^2 G(n,m,t-t')}{\partial t^2}$$

$$= -\frac{\delta(t-t')\delta_{nm}}{M} - \frac{1}{M}\sum_l \Phi(n,l)\,G(l,m,t-t')$$

$$- (2M)^{-1}\sum_{l,r}\Phi^{(3)}(n,l,r)\langle\langle u(l,t)u(r,t);u(m,t')\rangle\rangle, \quad \text{(A2)}$$

where we have used the equation of motion

$$\frac{\partial p(n)}{\partial t} = (i\hbar)^{-1}[p(n),H]$$

$$= -\sum_l \Phi(n,l)u(l) - \tfrac{1}{2}\sum_{l,r}\Phi^{(3)}(n,l,r)u(l)u(r),$$

which follows from (1) with the neglect of the quartic term (we neglect the quartic term at this point because it does not lead to important frequency structure at our stage of anharmonic approximation), and where $\delta(t-t')$ comes from differentiating the step function $\theta(t-t')$. The Fourier frequency components of Eq. (A2) satisfy the equation

$$\sum_l [M\omega^2\delta(n,l) - \Phi(n,l)]\,G(l,m,\omega)$$

$$= \delta_{nm} + \tfrac{1}{2}\sum_{l,r}\Phi^{(3)}(n,l,r)\langle\langle u(l)u(r);u(m)\rangle\rangle_\omega. \quad \text{(A3)}$$

To evaluate the last term on the right-hand side in (A3), we find the equation of motion of $\langle\langle u(l,t)u(r,t);u(m,t')\rangle\rangle$ by differentiating twice with respect to t', which gives

$$\frac{\partial^2}{\partial t'^2}\langle\langle u(l,t)u(r,t);u(m,t')\rangle\rangle$$

$$= M^{-1}[\langle u(l)\rangle_T\delta_{rm} + \langle u(r)\rangle_T\delta_{lm}]\,\delta(t-t')$$

$$- M^{-1}\sum_s\langle\langle u(l,t)u(r,t);u(s,t')\rangle\rangle\,\Phi(s,m)$$

$$- (2M)^{-1}\sum_{s,j} G^{(2)}(l,r;s,j,t-t')\,\Phi^{(3)}(s,j,m), \quad \text{(A4)}$$

where $G^{(2)}$ is defined by Eq. (8). We neglect the term in square brackets in (A4) which is propor-

tional to $\langle u \rangle$ and gives the thermal expansion. This term is generally nonzero with cubic anharmonicity but could be made to vanish by adjusting the lattice spacing self-consistently to account for thermal expansion; in any case, it is neglected here because it does not have a strong frequency dependence. Thus, the Fourier components of (A4) satisfy

$$\sum_s \langle\langle u(l)u(r);u(s)\rangle\rangle_\omega [M\omega^2\delta_{s,m} - \Phi(s,m)] = \tfrac{1}{2}\sum_{s,j} G^{(2)}(l,r;s,j,t-t')\Phi^{(3)}(s,j,m) \ . \quad \text{(A5)}$$

The substitution of (A5) into (A3) leads immediately to

$$\underline{G}(\omega) = \underline{g}(\omega) + \underline{g}(\omega)[\tfrac{1}{4}\underline{\Phi}^{(3)} : \underline{G}^{(2)}(\omega) : \underline{\Phi}^{(3)}]\underline{g}(\omega) \quad \text{(A6)}$$

in matrix notation, where $\underline{g}(\omega) = (\underline{M}\omega^2 - \underline{\Phi})^{-1}$ is the harmonic one-phonon Green's function. Clearly the quantity in square brackets in (A6) represents $T(\omega)$, the T matrix for scattering of phonons by cubic anharmonicities, and is exact (except for the thermal expansion). The self-energy $\Sigma(\omega)$ consists of the irreducible parts of $T(\omega)$. The lowest-order such part is simply $\frac{1}{4}\underline{\Phi}^{(3)} : \underline{g}^{(2)}(\omega) : \underline{\Phi}^{(3)}$, which gives the simple bubble diagram and Eq. (7).

The quartic phonon-phonon resonance of Eq. (23) can be obtained by considering the equation of motion of $G^{(2)}(\omega)$ in (A6), in the presence of quartic anharmonicities and keeping only those terms corresponding to the diagrams of Fig. 1(c).

APPENDIX B

The integral (16) can be evaluated in a straightforward manner by first rewriting the denominator of the integrand in the form

$$\Omega + \sin\tfrac{1}{2}k'a + \sin\tfrac{1}{2}(k-k')a = \Omega + (2C)^{1/2}\sin(\tfrac{1}{2}k'a + \theta), \quad \text{(B1)}$$

where $C = 1 - \cos(\frac{1}{2}\ a)$, and $\sin\theta = (\sin\frac{1}{2}ka)/(2C)^{1/2}$. Then we change variables letting $x = \frac{1}{2}k'a + \theta$, and with some manipulations obtain

$$I(k,\Omega) + I(k,-\Omega) = 2a^{-1}(2C)^{-1/2} \times\left[2(2C)^{1/2} + \frac{\Omega^2 - \sin^2\frac{1}{2}ka}{2C}\quad [J_k(\Omega) + J_k(-\Omega)]\right], \quad \text{(B2)}$$

where

$$J_k(\Omega) + J_k(-\Omega) = 2\int_\theta^{ka/2+\theta} \frac{dx\,\sin x}{\sin^2 x - \Omega^2(2C)^{-1}} = 2\int_{-\cos\theta}^{\cos\theta} \frac{du}{[1-\Omega^2(2C)^{-1}] - u^2} \ , \quad \text{(B3)}$$

which is logarithmic or an arctangent depending upon whether $\Omega^2 - 2C$ is less or greater than zero, respectively. The result can be found in any integral table and gives Eq. (17) immediately.

---

*Work supported in part by the National Science Foundation.

[1]V. V. Goldman, G. K. Horton, and M. L. Klein, Phys. Rev. Letters 24, 1424 (1970).

[2]H. Horner, Phys. Rev. Letters 25, 147 (1970).

[3]L. P. Pitaevskii, Zh. Eksperim. i Teor. Fiz. Pis'ma v Redaktsiyu 12, 118 (1970) [Sov. Phys. JETP Letters 12, 82 (1970)]; T. J. Greytak, R. Woerner, J. Yan, and R. Benjamin, Phys. Rev. Letters 25, 1547 (1970).

[4]M. H. Cohen and J. Ruvalds, Phys. Rev. Letters 23, 1378 (1969); J. Rubalds and A. Zawadowski, Phys. Rev. B 2, 1172 (1970); S. Solin and A. K. Ramdas, *ibid.* B 1, 1687 (1970).

[5]See, for example, D. N. Zubarev, Usp. Fiz. Nauk 71, 71 (1960) [Sov. Phys. Usp. 3, 320 (1960)].

[6]See, for example, A. A. Maradudin and A. E. Fein, Phys. Rev. 128, 2589 (1962); or R. A. Cowley, in *Phonons in Perfect Lattices and in Lattices with Point Imperfections*, edited by R. W. H. Stevenson (Oliver and Boyd, Edinburgh, Scotland, 1966).

[7]Essentially the same formula is obtained in the free-energy calculation of A. A. Maradudin, P. A. Flinn, and R. A. Colwell-Horsfall, Ann. Phys. (N. Y.) 15, 337 (1961).

[8]G. K. Horton and J. Lurie (private communication).

[9]H. J. Maris, Phys. Letters 17, 228 (1965).

[10]J. Minkiewicz (private communication).

[11]R. A. Cowley, Rept. Progr. Phys. 31, 123 (1968).

[12]J. F. Scott, Phys. Rev. Letters 21, 907 (1968).

[13]C. F. Coll, A. B. Harris, and A. J. Berlinsky, Phys. Rev. Letters 25, 858 (1970).

[14]See, for example, R. A. Cowley, Advan. Phys. 12, 421 (1963); or the articles by H. Bilz and J. R. Hardy, in *Phonons in Perfect Lattices and in Lattices with Point Imperfections*, edited by R. W. H. Stevenson (Oliver and Boyd, Edinburgh, Scotland, 1966).

[15]V. Ambegaokar, J. Conway, and G. Baym, in *Proceedings of the* 1963 *International Conference on Lattice Dynamics*, edited by R. F. Wallis (Pergamon, New York, 1964); and A. A. Maradudin and V. Ambegaokar, Phys. Rev. 135, A1071 (1964).

[16]J. Ruvalds (unpublished).